

Photoluminescence studies of spray pyrolytically grown nanostructured tin oxide semiconductor thin films on glass substrates

This content has been downloaded from IOPscience. Please scroll down to see the full text.

2006 J. Phys. D: Appl. Phys. 39 4540

(<http://iopscience.iop.org/0022-3727/39/21/004>)

View [the table of contents for this issue](#), or go to the [journal homepage](#) for more

Download details:

IP Address: 14.139.185.18

This content was downloaded on 07/08/2014 at 04:33

Please note that [terms and conditions apply](#).

# Photoluminescence studies of spray pyrolytically grown nanostructured tin oxide semiconductor thin films on glass substrates

Saji Chacko, M Junaid Bushiri<sup>1</sup> and V K Vaidyan

Department of Physics, University of Kerala, Kariavattom-695581, Kerala, India

E-mail: [junaidbushiri@gmail.com](mailto:junaidbushiri@gmail.com)

Received 28 July 2006, in final form 30 August 2006

Published 20 October 2006

Online at [stacks.iop.org/JPhysD/39/4540](http://stacks.iop.org/JPhysD/39/4540)

## Abstract

SnO<sub>2</sub> nanocrystalline thin films were deposited on glass substrates by the spray pyrolysis technique in air atmosphere at 375, 400, 425, 450 and 500 °C substrate temperatures. The obtained films were characterized by using XRD. The room temperature photoluminescence (PL) spectra of these films have near band edge (NBE) and deep level emission under the excitation of 325 nm radiation. NBE PL peak intensity decreased consistently with temperatures for samples prepared at 400, 450 and 500 °C, while a sudden reduction in intensity is observed for the sample prepared at 425 °C. A similar effect was observed for the optical transmittance spectra. These effects can be explained on the basis of the change in population of oxygen vacancies as indicated by the change in  $\Delta a$  values.

## 1. Introduction

Tin oxide is a wide band gap n-type semiconductor with a band width of 3.6 eV [1, 2]. SnO<sub>2</sub> with its qualities of being quite stable towards atmospheric conditions, chemically inert, mechanically hard and a material that can resist high temperatures is becoming more popular among the available transparent conducting oxide thin films. These properties of SnO<sub>2</sub> have aroused great interest in the development of a short wavelength semiconducting laser, which has potential application in manufacturing the next generation CD read heads, etc [2]. Recently, considerable investigation has been focused on the exploration of novel optical properties such as photoluminescence (PL) and electroluminescence of SnO<sub>2</sub> nanocrystalline thin films [3–6]. Generally, direct band gap semiconductors such as ZnO and SnO<sub>2</sub> have two emission peaks, a near band edge emission (NBE) (~3.14 eV) and a deep level emission (DLE) at higher wavelength (~2.2 eV) [2, 7, 8]. The NBE emission is due to excitons and intrinsic and extrinsic defects contribute to DLE [5, 9–14]. The surface state of materials play a crucial role in the emission characteristics of nanomaterials [14]. High crystallinity of nanostructure is

one of the most important factors in achieving a better NBE to DL emission ratio [2]. Spray pyrolysis with the added quality of being simple and economical in its experimental arrangement is used for the deposition of nanostructured thin films. It also has the advantages like ease of adding doping material, reproducibility, high growth rate and mass production capability [15]. In this communication, we report the PL characteristics of spray pyrolytically deposited nanostructured SnO<sub>2</sub> thin films on glass substrates.

## 2. Experimental

SnO<sub>2</sub> nanofilms were prepared by the spray pyrolysis technique. 0.1 M hydro ethanolic solution was prepared by dissolving SnCl<sub>4</sub>.5H<sub>2</sub>O in a mixture of absolute ethanol and high purity H<sub>2</sub>O in the ratio 1 : 1. A few drops of concentrated HCl were also added to the precursor solution. The solution was sprayed using a spray-rate controlled atomizer (40 mL min<sup>-1</sup>) on glass substrates (1 mm thick) placed over a temperature controllable oven in air atmosphere. The time of deposition was 90 s. The films were prepared at different substrate temperatures 375 (sample A), 400 (B), 425 (C), 450 (D) and 500 °C (E). The experiment was repeated by

<sup>1</sup> Author to whom any correspondence should be addressed.

changing the deposition time to 2 min and films were prepared at different substrate temperatures of 400 (sample P), 425 (Q) and 450 °C (R). PL spectra of the samples were recorded with a SPEX Fluorolog fluorescence spectrophotometer using a 325 nm line of a Xe lamp as an excitation source. The XRD pattern of the films were obtained from a Philips 1830 x-ray diffraction spectrometer using  $\text{CuK}\alpha_1$  (1.540 56 Å) radiation.

### 3. Results and discussion

The x-ray diffraction patterns of the samples prepared at different temperatures are shown in figure 1. The XRD patterns of the films prepared at and above 400 °C reveal that these films are polycrystalline in nature. Tin oxide crystal nucleation started at 400 °C and attained  $\text{SnO}_2$  structure as can be seen from the x-ray diffraction pattern. The diffraction pattern of the sample A has no peaks which indicate the amorphous nature of the film. This film shows electrical conductivity which confirms the formation of the tin oxide amorphous phase. In sample B, randomly oriented tin oxide crystalline formation starts and planes corresponding to (110), (101), (200) and (211) appear with very weak intensities. The presence of broad and weak peaks indicates that  $\text{SnO}_2$  has a very small crystalline size or that  $\text{SnO}_2$  particles are semicrystalline in nature [12]. The peak intensity of the (200) plane increases when the substrate temperature is raised to 425 °C and shows a preferential orientation. All other peaks corresponding to other planes appeared with very weak intensities. It is found that the XRD peaks become gradually sharper with temperature,

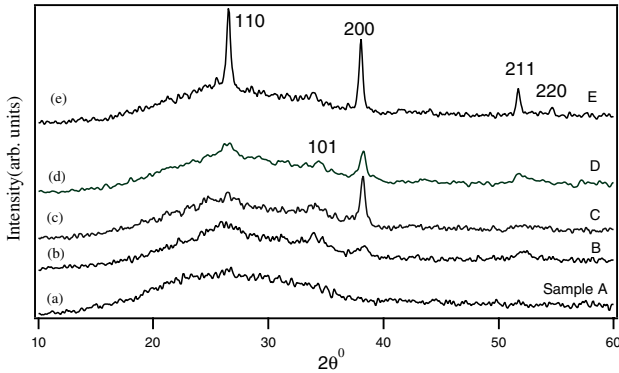


**Figure 1.** XRD patterns of spray pyrolytically grown nanocrystalline  $\text{SnO}_2$  thin films with a deposition time of 90 s at different substrate temperatures (a) 375, (b) 400, (c) 425, (d) 450 and (e) 500 °C.

**Table 1.** Relationship of lattice parameters for different samples.  $a_{110}$  and  $a_{200}$  are calculated with XRD peaks (110) and (200) and  $c_{101-110}$  and  $c_{101-200}$  are calculated with XRD peaks (101), (110) and (200), respectively.

Lattice parameters	Powder sample [32]	As-prepared samples				Commercial bulk
		Sample B (400 °C)	Sample C (425 °C)	Sample D (450 °C)	Sample E (500 °C)	
$a_{110}$ (Å)	4.733	4.8216	4.7200	4.7573	4.7418	4.727
$a_{200}$ (Å)	4.738	4.7138	4.7068	4.6975	4.7272	4.732
$\Delta a$ (Å)	-0.005	0.1078	0.0132	0.0598	0.0146	-0.005
$c_{101-110}$ (Å)	3.186	3.1574	3.1648	3.1093	3.2120	3.173
$c_{101-200}$ (Å)	3.184	3.1892	3.1686	3.1265	3.2165	3.172
$\Delta c$ (Å)	0.002	-0.0318	-0.0038	-0.01714	-0.0045	0.001

indicating a larger particle size. Intensities corresponding to (110), (101) and (211) get enhanced with temperature showing better crystallinity of films deposited at higher temperature, in agreement with previous studies [3, 16, 17]. In sample E, an enhanced intensity shift towards (110) from (200) plane and a new peak corresponding to (220) plane appears.

The presence of a large number of vacant lattice sites and local lattice disorders may lead to an obvious reduction or even disappearance in intensities of XRD peaks corresponding to lattice planes such as (220), (002), (202) and (112). The disappearance and reduction in intensities of XRD peaks of some lattice planes imply the presence of a large number of vacant lattice sites, destroyed periodicities in some crystal planes and local lattice disorders [6]. The  $\text{SnO}_2$  films deposited by spray pyrolysis technique are more susceptible to oxygen deficiencies [16, 18–23]. We have calculated the lattice parameters of as-prepared  $\text{SnO}_2$  thin films and are given in table 1. It is found that there are changes in lattice parameters, when compared with  $\text{SnO}_2$  bulk, an increase in  $a$  and decrease in  $c$  for the as-prepared  $\text{SnO}_2$  nanocrystalline thin films. This implies that the as-prepared thin films may exhibit a large number of oxygen vacancies, vacancy clusters and local lattice disorders, which lead to an increase in  $a$  ( $\Delta a$ ) and a decrease in  $c$  ( $\Delta c$ ) [6]. Thus, change in unit cell parameters  $a$  ( $\Delta a$ ) and in  $c$  ( $\Delta c$ ) is a measure of population of oxygen vacancies. Thus, we define

$$\Delta a = a_{110} - a_{200}, \quad (1)$$

$$\Delta c = c_{101-110} - c_{101-200}. \quad (2)$$

The PL spectra of the samples prepared with deposition time 90 s at different substrate temperatures are shown in figure 2. The inset shows the PL spectrum of sample A. The photoemission spectra of the sample A prepared at a substrate temperature of 375 °C has emission peaks at 395, 435, 546 and 578 nm. The x-ray diffraction pattern of sample A indicates poor crystalline nature (figure 1). This may be due to deviation from stoichiometry and structure defects [24]. This film probably has more intrinsic defects especially oxygen vacancies. This can trap the electrons from the valence band and can act as luminescent centres [13]. The NBE emission observed at 395 nm is due to a recombination of deep trapped charges and photogenerated electrons from the conduction band [5, 9–12]. The observed PL peak at 546 nm is contributed by singly ionized charge state of oxygen [25–29]. The sharp violet emission peak (435 nm) can be ascribed to luminescence centres formed by tin interstitials or dangling [5, 30]. The yellow emission band at 578 nm (trap emission)

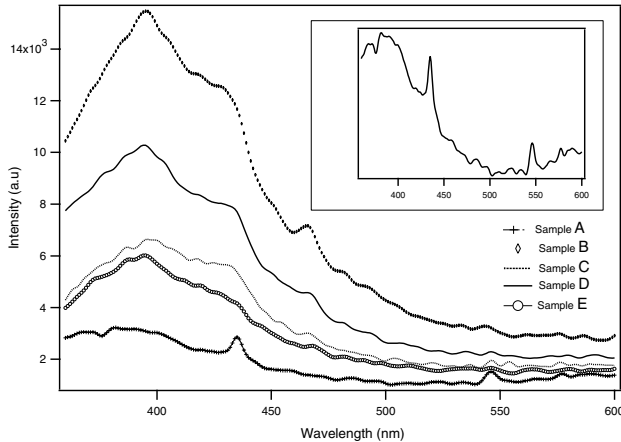


**Figure 2.** Room temperature PL spectra of spray pyrolytically grown nanocrystalline SnO<sub>2</sub> thin films with a deposition time 90 s. The inset shows the PL spectrum of sample A.

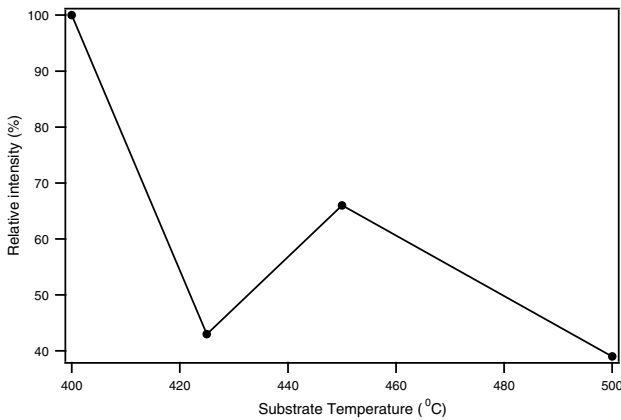


**Figure 3.** The variation of NBE emission intensity with substrate temperatures.

can be attributed to defect levels in the band gap as reported by Cai *et al* [13].

The PL spectrum of sample B shows a broad emission peak at 395 nm followed by a weak shoulder at 433 nm. A new peak is observed in the emission spectrum of this film at 466 nm [29]. The films prepared at relatively higher substrate temperatures (425, 450 and 500 °C) have a broad photoemission peak centred around 395 nm. The formation of these films in air atmosphere reduces the possibility of defect population (such as oxygen and excess tin), thus encouraging the formation of stoichiometrically better films. This will lead to a relatively weaker DLE (defect induced) in samples prepared at higher substrate temperatures (450 and 500 °C). Good crystalline nature of the material can be attributed to high NBE-to-DLE intensity ratio, resulting in detectable near-UV emission at room temperature [2]. The peak intensities contributed by defects in the crystalline systems at 466 nm and the shoulder at 433 nm gradually diminish with the increase in substrate temperature [29]. This confirms the improvement of crystallinity and rules out the presence of Sn interstitials in agreement with the x-ray diffraction pattern.

It is interesting to note that NBE emission peak intensity is comparatively low for sample A. While it is maximum for sample B (figure 3). Emission intensity rapidly decreases

for sample C. While for sample D, it improves [14, 30]. Again, the emission intensity decreases for sample E. The PL emission efficiency is determined by the ratio of radiative and nonradiative transitions. The nonradiative transition is induced by crystal imperfections such as point defects, dislocations and grain boundaries. The radiative transitions are composed of two parts: NBE excitonic related UV emission and DLE [14]. The excitonic emissions are more sensitive to imperfections and particle size in a crystal. The increased grain size favours the decrease of the concentration of nonradiative recombination centres. However, at the same time, high temperature increases the probability of formation of radiative defects, which will compete with excitonic recombination and decrease UV emission efficiency [14].

In the present study, we found that the particle size increases with substrate temperature. The particle size was calculated by the Scherrer equation [12, 14]. The variation of particle size with substrate temperature, NBE emission peak relative intensity percentage, transmittance near to solar maximum (550 nm) and change in lattice parameters along with commercial bulk values of SnO<sub>2</sub> are given in table 2 [17]. Intensity that decreases with increase in substrate temperature is in good agreement with previous studies [5, 14, 28]. However, we observed a reduction in NBE emission intensity at a substrate temperature of 425 °C which is not in agreement with the general pattern. From the XRD pattern we observed a preferential orientation for sample C in the (200) direction.

The increase in lattice parameter  $a$  and decrease in  $c$  (table 2) show an increase in oxygen vacancies, that will lead the recombination of deep trapped charges and photogenerated electrons from the conduction band. The intensity of the peak thus increases with concentration of oxygen vacancies [3]. The observed variation in PL emission intensity with the change of thin film deposition substrate temperature can be explained as being due to the concentration of oxygen vacancies and local lattice disorders, which can be correlated to the change in unit cell parameters  $a$  ( $\Delta a$ ) and  $c$  ( $\Delta c$ ). The PL NBE emission intensity is found to be maximum for the sample having a maximum value of  $\Delta a$  (table 2). We observed a similar effect for transmittance spectra of these samples. The transmittance spectra of the samples also show a dependence on the variation of lattice parameters. Sample C has a maximum transmittance at 550 nm (96 %) which has a minimum  $\Delta a$ . The decrease in lattice disorder due to the reduction of population density of oxygen vacancies enhances the crystalline nature of the films. This in turn improves the transmittance percentage. It is previously reported that the (200) preferred crystalline film shows an average transmittance of 92% in the visible region [31]. Thus, it can be seen from these observations that NBE PL intensities and optical transmittance of spray pyrolytically grown SnO<sub>2</sub> nanocrystalline thin films depend on the crystalline nature of the samples and can be hence explained as a function of change in lattice parameters.

#### 4. Conclusions

The PL characteristics of spray pyrolytically deposited nanostructured SnO<sub>2</sub> thin films on glass substrates are reported for the first time. The room temperature PL spectra of these

**Table 2.** Particle size (nanometres) NBE emission (395 nm) intensity (%) and transmittance (%) of spray pyrolytically grown SnO<sub>2</sub> thin films at different substrate temperatures and spray time.

Sample	Substrate temperature (°C)	Particle size (nm)	$\Delta a$	$\Delta c$	NBE emission (395 nm) relative intensity (%)	Transmittance at 550 nm (%)
A	375	Poor crystalline			25	88
B	400	6	0.108	-0.032	100	65
C	425	15	0.013	-0.004	43	96
D	450	17	0.06	-0.017	66	68
E	500	29	0.015	-0.005	39	78

films have NBE and DLE under the excitation of 325 nm radiation. The NBE emission observed at 395 nm is due to the recombination of photogenerated free excitons between the conduction band and valence band. NBE PL peak intensity decreased consistently with temperatures for samples prepared at 400, 450 and 500 °C, while a sudden reduction in intensity is observed for the sample prepared at 425 °C. A similar effect was observed for the optical transmittance spectra. These effects can be explained on the basis of the change in population of oxygen vacancies as indicated by the change in  $\Delta a$  values.

### Acknowledgment

Saji Chacko is grateful to the University Grants Commission, New Delhi, for the award of a Teacher Fellowship under the X plan.

### References

- [1] He J H, Wu T H, Hsin C L, Li K M, Chen L J, Chueh Y L, Chou L J and Wang Z L 2006 *Small* **2** 116
- [2] Cao H, Qiu X, Liang Y, Zhang L, Zhao M and Zhu Q 2006 *Chem. Phys. Chem.* **7** 497
- [3] Jeong J, Choi S P, Chang C I, Shin D C, Park J S, Lee B-T, Park Y-J and Song H-J 2003 *Solid State Communs.* **127** 595
- [4] Kim T W, Lee D U and Yoon Y S 2000 *J. Appl. Phys.* **88** 3759
- [5] Gu F, Wang S F, Lu M K, Cheng X F, Liu S W, Zhou G J, Xu D and Yuan D R 2004 *J. Cryst. Growth* **262** 182
- [6] Chen Z W, Lai J K L and Shek C H 2004 *Phys. Rev. B* **70** 165314
- [7] Im S, Jin B J and Yi S 2000 *J. Appl. Phys.* **87** 4558
- [8] Chen S J, Liu Y C, Lu Y M, Zhang J Y, Shen D Z and Fan X W 2006 *J. Cryst. Growth* **289** 55
- [9] Reynolds D C, Look D C, Jobai B, Litton C W, Collins T C, Harsch W and Cantwell G 1998 *Phys. Rev. B* **57** 12151
- [10] Hopfield J J and Thomas D G 1961 *Phys. Rev.* **122** 35
- [11] Kong Y C, Yu D P, Zhang B, Fang W and Feng S Q 2001 *Appl. Phys. Lett.* **78** 407
- [12] Gu F, Wang S F, Lu M K, Zhou G J, Xu D and Yuan D R 2004 *J. Phys. Chem. B* **108** 8119
- [13] Cai D, Su Y, Chen Y, Jiang J, He Z and Chen L 2005 *Mater. Lett.* **59** 1984
- [14] Wang Y G, Lau S P, Lee H W, Yu S F, Tay B K, Zhang X H and Hng H H 2003 *J. Appl. Phys.* **94** 354
- [15] Elangoavn E and Ramamurthi K 2005 *Thin Solid Films* **476** 231
- [16] Sumangala Devi Amma D, Vaidyan V K and Manoj P K 2005 *Mater. Chem. Phys.* **93** 194
- [17] Shanthi S, Subramanian C and Ramasamy P 1999 *J. Cryst. Growth* **197** 858
- [18] Bruneaux J, Cachet H, Froment M and Massad A 1991 *Thin Solid Films* **197** 129
- [19] Rakshani A E, Makdisi Y H A and Ramazanyan H A 1998 *J. Appl. Phys.* **83** 1049
- [20] Fantini M and Torriani I 1986 *Thin Solid Films* **138** 255
- [21] Shanthi E, Datta V, Banerjee A and Chopra K L 1980 *J. Appl. Phys.* **51** 6243
- [22] Shanthi E, Datta V, Banerjee A and Chopra K L 1982 *Thin Solid Films* **88** 93
- [23] Patil P S, Kawar R K, Seth T, Amalnerkar D P and Chigare P S 2003 *Ceram. Int.* **29** 725
- [24] Alterkop B, Parkansky N, Goldsmith S and Boxman R L 2003 *Appl. Phys.* **36** 552
- [25] Vanheusden K, Seager C H, Warren W L, Tallant D L and Voigt J A 1996 *Appl. Phys. Lett.* **68** 403
- [26] Vanheusden K, Warren W L, Seager C H, Tallant D R, Voigt J A and Gnade B E 1996 *J. Appl. Phys.* **79** 7983
- [27] Egelhaaf H J and Delkrug D 1996 *J. Cryst. Growth* **161** 190
- [28] Meng X Q, Shen D Z, Zhang J Y, Zhao O X, Dong L, Lu Y M, Liu Y C and Fan X W 2005 *Nanotechnology* **16** 609
- [29] Luo S, Fan J, Liu W, Zhang M, Song Z, Lin C, Wu X and Chu P K 2006 *Nanotechnology* **17** 1695
- [30] Gu F, Wang S F, Song C F, Lu M K, Qi Y X, Zhou G J, Xu D and Yuan D R 2003 *Chem. Phys. Lett.* **372** 451
- [31] Fukano T and Motohiro T 2004 *Sol. Energy Mater. Sol. Cells* **82** 567
- [32] McCarthy G and Welton J 1989 *Powder Diffract.* **4** 156